Role of Traf3 in Anxiety-Like Behavior and Fear Response

Vivian Sanchez Neyra

Department of Neuroscience, Tufts University

Bygrave Laboratory

Lina Oh, Dr. Alexei Bygrave

September 21, 2026

Abstract

Psychiatric disorders present a major global health challenge, yet the underlying biological mechanisms behind them remain under researched and thus, poorly understood. Genome-wide association studies have linked Tumor Necrosis Factor Receptor-Associated Factor 3 (Traf3) to major depressive disorder, post-traumatic stress disorder, and suicidal ideation, though its specific role in neural circuitry is unknown. Traf3 was proven to be enriched at excitatory synapses of inhibitory interneurons by postsynaptic protein profiling. Moreover, the knock-out (KO) of Traf3 from all inhibitory neurons (vGat-Traf3 KO) lead to heightened anxiety-like and depressive-like phenotypes, as well as increased fear response during fear conditioning. However, this vGat-Traf3 KO line is a very broad knockout, including many different subtypes of inhibitory interneurons. Therefore, in this study, we investigated whether the behavioral differences are driven by Parvalbumin (PV)-expressing interneurons specifically. We used a conditional PV-Traf3 KO mouse line to evaluate baseline anxiety and associative fear learning and memory using the Open Field Test, Elevated Plus Maze, and cued fear conditioning extinction paradigms. Contrary to the broad vGat-Traf3 phenotype, PV-Traf3 KO mice exhibited no significant differences from the control group in any of these evaluations ($P > 0.05$). These results indicate that Traf3 expression specifically within PV interneurons is not required to display an increased anxiety-like phenotype or increased fear learning. The discrepancy between the two knock-out models suggests that the phenotypes seen in broad GABAergic Traf3 (vGat-Traf3) knockouts can be attributed to Traf3 function in another or a combination of GABAergic interneuron subtypes.

Introduction

Psychiatric disorders have been a growing global public health crisis. Over 30% to 40% of US adults reported symptoms of anxiety or depression during peak periods of the COVID-19 pandemic (Mark & Eacute et al. 2020). Alarmingly, the suicide rate in the United States has increased by approximately 35% over the past two decades (CDC, 2020). Despite the unfortunate prevalence of these conditions, current treatment options remain limited in reliability. Between 30-55% of individuals receiving antidepressant treatment experience treatment-resistant depression (McIntyre et al. 2023), leading to a critical need for more effective and targeted approaches. These must come from a deeper understanding of the underlying genetic mechanisms that contribute to symptom expression.

Previous studies have shown how the dysfunction of interneurons, which control the neural network activity in the brain, leads to an imbalance in neural circuits, which has been implicated in the pathophysiology of psychiatric disorders. Inhibitory interneurons (INs) make up a minority of the brain's neuronal population and represent a diverse population of neurons. As GABAergic neurons, INs tightly regulate the activity of surrounding neurons, making INs of great interest when researching psychiatric disorders. Accordingly, large-scale genome wide association studies have begun to identify specific IN genes that may be involved in psychiatric disorder susceptibility. Among these, Tumor Necrosis Factor Receptor-Associated Factor 3 (Traf3) has stood out as a gene with likely risk for major depressive disorder (MDD), suicide, and PTSD, though its biological basis remains unknown.

Background

INs are a small and diverse group of GABAergic neurons, which produce the brain's main inhibitory neurotransmitter, GABA. INs tightly regulate the activity of the PNs and are

identified based on the presence of Vesicular GABA Transporter (vGat), a marker of inhibitory neurons. There are different types of INs, such as vasoactive intestinal peptide-expressing (VIP) neurons, somatostatin-expressing (SST), as well as parvalbumin-expressing (PV) neurons. These differ by the location they each target and their interaction style; for example, PV INs synapse on the soma and proximal dendrites of pyramidal cells and they provide powerful, fast-spiking, global shunting inhibition to control overall action potential output. Whereas SST INs target distal dendrites and they selectively modulate specific clusters of synaptic inputs arriving at the dendrites rather than shutting down the whole cell (Fishell and Kepecs 2020), as observed on Figure 1.

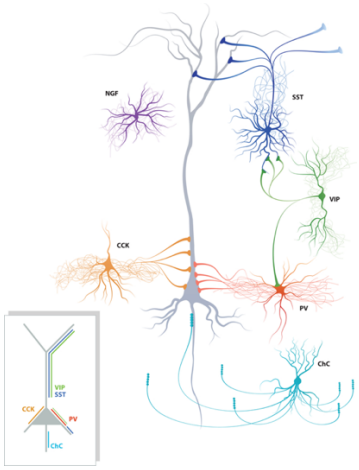

Figure 1. *A few major classes of interneurons are shown. Somatically targeting neurons can be classified into two large classes of PV- or cholecystokinin (CCK)-expressing basket cells. SST interneurons form synapses on dendrites, while VIP-expressing interneurons target mainly SST and, to a lesser degree, PV interneurons. Inset shows depiction of interneuron targeting pyramidal cells. Taken from Fishell and Kepecs, 2020.*

Something that is less known about INs is the postsynaptic composition at their glutamatergic synapses, which allow INs to become depolarized and thus release GABA to suppress nerve cell firing. A new protein was identified in these synapses by Dr. Bygrave's

postdoctoral work, which conducted an unbiased proteomic characterization of the proteins in complex with Psd-95, which is the scaffolding protein in postsynaptic density of glutamatergic synapses (Bygrave et al. 2023).This was done by breeding conditional Psd-95-GFP knockin mice with vGat- or CaMKII-Cre animals. Psd-95-GFP mice express a green fluorescent protein (GFP) attached to the Psd-95 protein, whereas vGat and CaMKII-Cre animals mark for inhibitory GABAergic neurons and excitatory glutamatergic neurons (ENs), respectively. By breeding these two transgenic mouse lines and observing the cortex and hippocampus (HPC) the Psd complexes preferentially originating from INs or ENs were identified. In the HPC and cortex, the population of vGat-expressing neurons are virtually all interneurons and thus referred to as INs. By normalizing to the amount of Psd-95, we found proteins that were specifically enriched in INs, as seen in Figure 2.

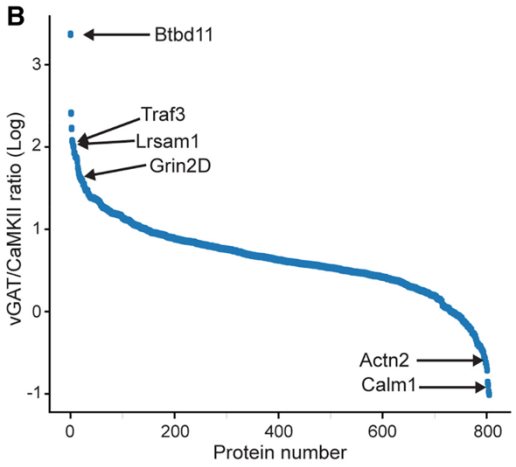

Figure 2. *Identification of Traf3 as an inPsd protein. Mass spectrometry data from postsynaptic density protein 95 (Psd-95) complex pull-down from vGat-expressing (inhibitory) and CaMKII-expressing (excitatory) cells showed that Traf3 is enriched in inhibitory neurons compared to excitatory neurons. All the protein values on the Y-axis were normalized to PSD-95 levels. Taken from Bygrave et al., 2023.*

Through postsynaptic protein profiling, Dr. Bygrave and his team identified Traf3, as a novel protein heavily enriched at these glutamatergic synapses of INs. Traf3 has stood out as a gene with likely risk for psychiatric disorders, but the possible biological mechanism underlying this hypothesis remains unknown. Traf3 is a stable protein (Heo et al. 2026) and has been primarily researched as a signaling molecule involved in immune pathways. More specifically, in the context of injury and inflammatory responses following hemorrhage and spinal injury (Luo et al. 2024), and it has been shown to regulate neural apoptosis (Zhou et al. 2021). Moreover, genome-wide association studies using human samples have identified single-nucleotide polymorphisms and differential Traf3 gene expression associated with psychiatric disorders and related behaviors. These include major depression disorder (MDD) (Levey et al. 2021), post-traumatic disorder (PTSD) (Nievergelt et al. 2024), and suicide ideation (Kimbrel et al. 2023). These have given the Bygrave Lab enough reason to suspect there might be behavioral deficits when Traf3 expression is disrupted.

Preliminary Data

The Bygrave Lab has been working to better understand Traf3 under the context of neurobiology and psychiatric applications.

To demonstrate Traf3 was enriched at inhibitory neurons, the lab used tissue from both control and vGat-Traf3 knock out (KO) mice, in which Traf3 was knocked out in neurons expressing the vGat promoter. Key fear circuitry regions in the brain, such as the basolateral amygdala (BLA), prefrontal cortex (PFC), and HPC, were analyzed. As seen in Figure 3, this KO of Traf3 in all inhibitory neurons leads to a significantly reduced overall expression of Traf3. This confirmed that Traf3 was knocked out successfully and, more importantly, that the gene is enriched at INs compared to the excitatory neurons in these key areas.

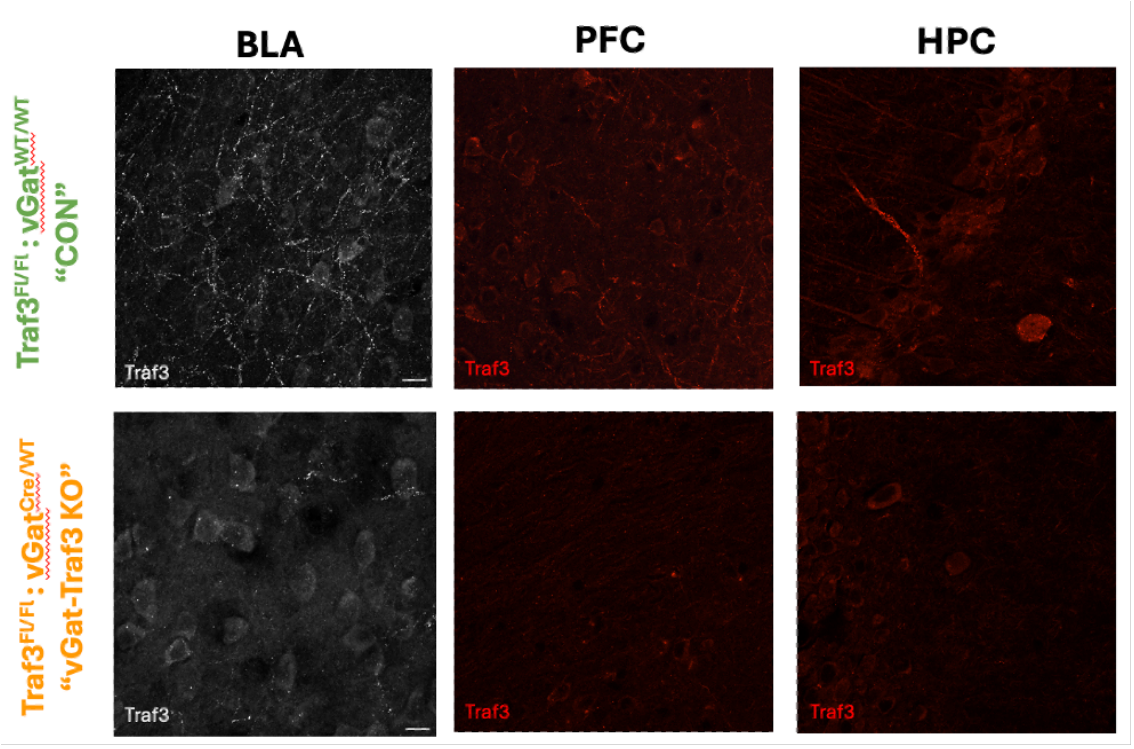

Figure 3. *Traf3 expression in control and vGat-Traf3 knockout mice. Representative immunohistochemistry (IHC) images showing Traf3 expression in the BLA, PFC, and HPC of control (CON, top row) and vGat-Traf3 knockout mice (KO, bottom row). Traf3 is shown in white in the BLA and red in the PFC and HPC.*

Moreover, to show that Traf3 is enriched at excitatory glutamatergic synapses, immunohistochemistry (IHC) microscopy combined with co-localization analysis was conducted in brain slices in the amygdala. Brain tissue sections were stained using primary bodies against Traf3 and Gephryn. These were then fluorescently labeled to visualize each protein channel under a high-resolution confocal microscope. As seen in Figure 4, specific dendritic segments were mapped, and Traf3 was found to be co-localized with Psd-95 and almost never with Gephyrin, the scaffolding protein in postsynaptic density of GABAergic synapses. This indicates that Traf3 expression is specific to glutamatergic synapses.

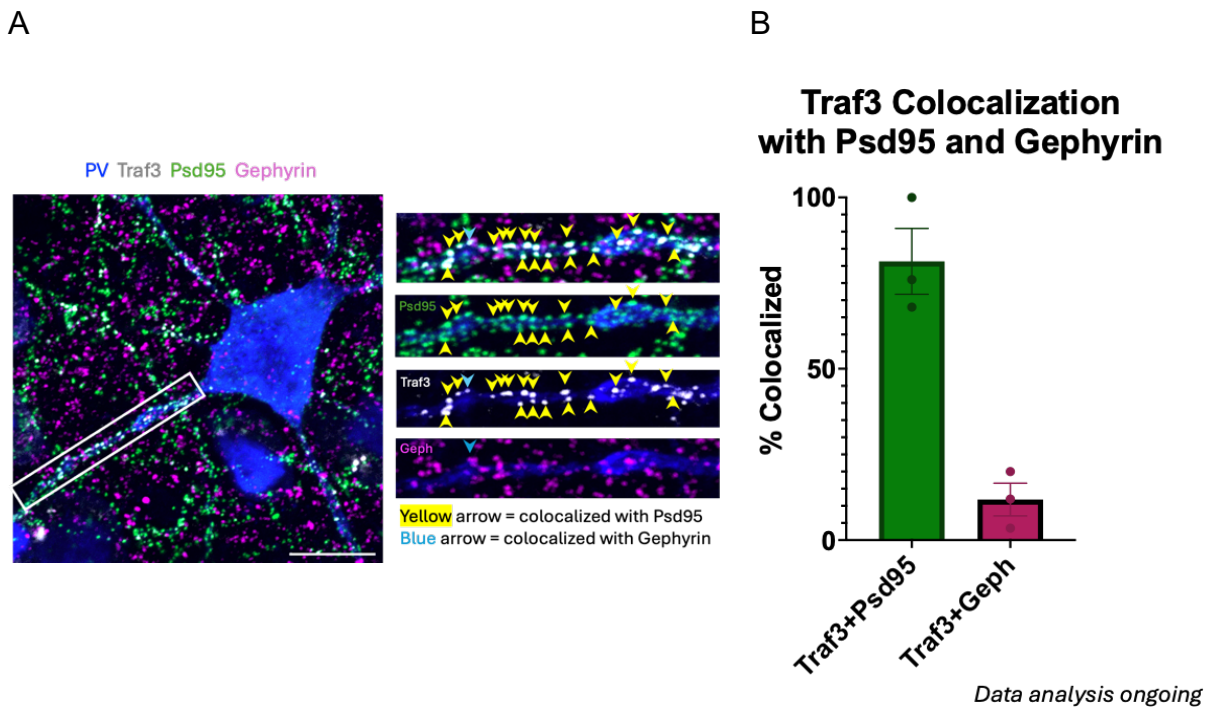

Figure 4. *Traf3 Colocalization with Psd-95 and Gephyrin. (A) IHC images showing the localization of Traf3 in gray, parvalbumin (PV) in blue, Psd-95 in green, and gephyrin (Geph) in magenta. The left panel shows a PV-expressing interneuron and surrounding synaptic markers, with the boxed region enlarged on the right. Enlarged panels show the individual Psd-95, Traf3, and gephyrin channels. Yellow arrowheads highlight puncta showing colocalization of Traf3 with Psd-95. Blue arrowheads highlight puncta showing colocalization of Traf3 with gephyrin. (B) Bar graph showing colocalization of Traf3 with Psd-95 vs its colocalization with Gephyrin.*

The lab worked with a mouse line with conditional knock-out of Traf3 under the vGat promoter (vGat-Traf3 KO), which knocks out Traf3 only in vGat-expressing inhibitory neurons, and conducted a range of behavioral tasks. The vGat-Traf3 KO and control mice underwent a series of experiments, such as the Open Field Test (OFT) and the Elevated Plus Maze (EPM). As seen in Figure 5, the vGat-Traf3 KO mice displayed greater anxiety-like behavior compared to the control group in both the OFT and EPM. The Tail Suspension Test showed that the KO mice

spent noticeably longer time immobile compared to the controls. This is interpreted in rodent models as a depressive-like symptom. Both control and KO mice did not show any changes in their motor or reward systems during the Rotarod Test and the Sucrose Preference Test, respectively (data not shown). This suggests that, in vGat-expressing neurons, Traf3 plays a significant role in regulating mood and emotional states, without affecting baseline motor functions or reward-seeking behaviors.

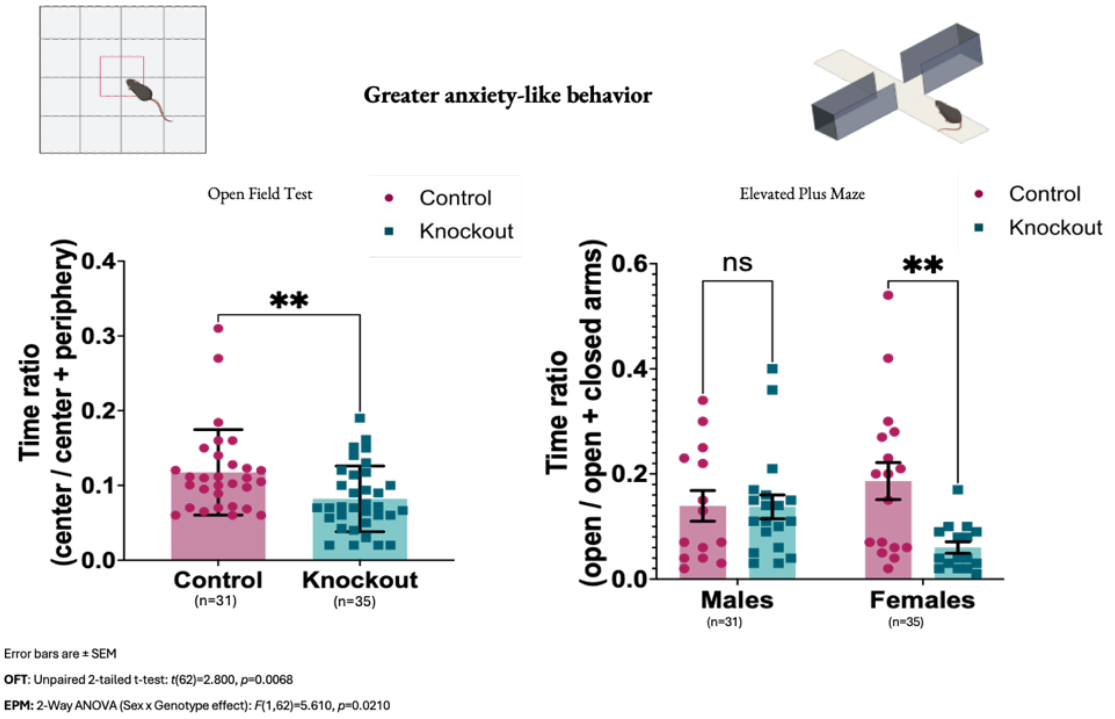

Figure 5. *Behavioral performance of control and vGat-Traf3 knockout mice. The data on the left show the comparison of behavior during the OFT, data on the right show the comparison during the EPM. Individual data points represent individual mice, with bars showing group means and error bars representing variability within each group.*

Finally, fear conditioning tests were conducted using a new set of vGat-Traf3 KO mice. These KO mice showed greater levels of freezing on the conditioning day and slightly less so but still freezing a little more on the first day of recall, displayed on Figure 6.

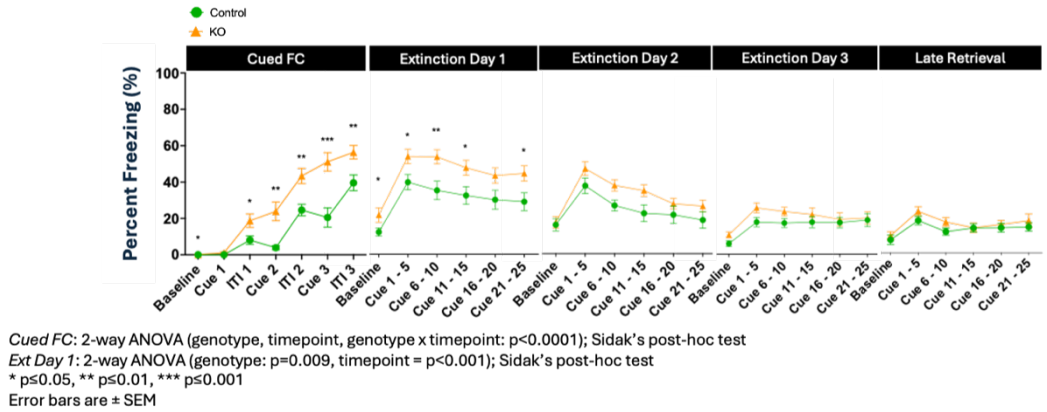

Cued FC: 2-way ANOVA (genotype, timepoint, genotype x timepoint: p<0.0001); Sidak's post-hoc test
Ext Day 1: 2-way ANOVA (genotype: p=0.009, timepoint = p<0.001); Sidak's post-hoc test
* p≤0.05, ** p≤0.01, *** p≤0.001
Error bars are ± SEM

Figure 6. *Fear conditioning and extinction in control and vGat-Traf3 knockout mice. The panel shows the percentage of freezing in both control and knockout mice during cued fear conditioning (Cued FC), 3 consecutive extinction days, and late retrieval. Each point represents the mean percentage of freezing with error bars showing variability. Asterisks above the data represent statistically significant differences ($p < 0.05$, $p << 0.01$, and $p <<< 0.001$) between the two groups.*

Neurons expressing vGat are composed of a highly diverse population of cells, including PV, SST, and VIP subtypes, each with their own circuit innervation patterns. While previous work in the lab demonstrates that a pan-inhibitory knockout of Traf3 (vGat-Traf3 KO) induces anxiety-like and depression-like phenotypes, it is hard to infer the circuit mechanisms underlying these phenotypes. Therefore, the aim of this project was to determine whether these behavioral alterations are driven by a specific interneuron subtype: namely, parvalbumin-expressing (PV) neurons, which constitutes the biggest population of INs.

Methods

PV-Traf3 KO

To investigate the cell-type-specific role of Traf3, we used a novel conditional KO mouse line featuring the targeted deletion of Traf3 exclusively within parvalbumin-expressing

interneurons (PV INs). This line was generated using the Cre-loxP recombinase system by crossing a tissue-specific PV-Cre driver line with a floxed Traf3 line. In the driver line, Cre recombinase is knocked in under the control of the endogenous Pvalb promoter, ensuring Cre expression is strictly restricted to active PV INs - which, as mentioned, are predominately fast-spiking GABAergic inhibitory interneurons in the brain. The floxed line harbors loxP sites flanking essential coding exons of the *Traf3* gene, preserving normal protein function until recombination occurs. The final mouse lines used were the control (Pvalb <WT/WT> ; Traf3 <FL/FL>) and the knockout line (Pvalb<tm1(cre)Arbr/WT>;Traf3 <FL/FL>). Mice were tested at 12-weeks-old and were handled for one week prior to the behavioral battery.

Open Field Test

Baseline locomotor activity and anxiety-like behavior were assessed using the Open Field Test. Each mouse was placed in the center of a square 406 x 406 x 380 mm chamber and allowed to freely explore for 10 minutes. Automated behavioral detection measured the percentage of time spent in the center (230 x 230 mm) versus the periphery. The total distance traveled (in) was quantified to measure locomotor function, and the ratio of time spent in the designated central zone was measured as an index of anxiety-like behavior. The apparatus was thoroughly cleaned with Chlorine Dioxide (ClO2) between subjects to eliminate olfactory cues. A lower ratio of time spent in the center of the arena was interpreted as increased anxiety-like behavior.

Elevated Plus Maze

Anxiety-like behavior was further evaluated using the Elevated Plus Maze. Each mouse was placed in the center of an elevated plus maze (EPM) and allowed to explore the maze for 5 minutes. The dimensions of the center of the EPM were 62 x 62 mm, while each arm measured 350 x 62 mm with a closed-arm wall height of 152 mm. Automated behavioral detection

measured the percentage of total time spent in the open arms. The maze was cleaned with ClO2 between each trial to eliminate any olfactory cues from the previous subject. A lower ratio of time spent in the open arms was interpreted as increased anxiety-like behavior.

Fear Conditioning

Fear conditioning is performed after the OFT and EPM because it involves an aversive stimulus that induces a profound stress state, which could otherwise invalidate subsequent tests. There was a waiting period of at least 1 week between the end of EPM and cued fear conditioning experiments.

To assess associative fear memory, mice underwent a cued fear conditioning presented in Figure 7. The conditioned context was a cubic chamber with a metal grid floor measuring 255 x 285 x 290 mm (measurements without grid floor: 255 x 285 x 325 mm). A higher frequency or longer duration of observed freezing behavior was interpreted as increased anxiety-like behavior. Videos were acquired using the FreezeFrame (Actimetrics) software.

Figure 7. *Fear conditioning and extinction paradigm. Schematic illustrates the fear conditioning and extinction paradigm followed by each mouse in the study.*

On Day 1, Cued Fear Conditioning (Context A) was performed. Following a 90-second baseline acclimation period, mice are exposed to 3 pairings of an auditory cue (tone) co-

terminating with a mild foot shock (0.6 mA). The trials are separated by variable inter-trial intervals (ITI 1: 60s, ITI 2: 90s, ITI 3: 120s).

Separated by 1-day intervals, mice undergo three consecutive days of fear extinction training in a novel environmental context (Context B) to alter visual, tactile, and olfactory cues. Each daily extinction session begins with a 90s baseline, followed by 25 presentations of the tone alone (no foot shock) separated by a fixed 60s ITI, concluding with a 90s cooldown period.

Finally on Day 18, to assess the long-term persistence or spontaneous recovery of the fear memory, mice are returned to Context B after a 14-day incubation period. This final late retrieval session follows the same parameters of an extinction session as listed in the previous paragraph (90s baseline, 25 tone-alone presentations with a 60s ITI, and a 90s cooldown).

Statistical Analysis

GraphPad Prism (v11) was used for all statistical analysis. Data were first evaluated for normality and lognormality. Data demonstrating a lognormal distribution were analyzed using a lognormal Welch's t-test to assess statistical significance between groups. Data meeting normal distribution assumptions were analyzed using a standard unpaired t-test, whereas non-parametric data were evaluated using a Mann-Whitney test. Group comparisons were then evaluated using a two-way ANOVA. Statistical significance was defined as $p < 0.05$.

Results

Open Field Test

We did not observe any statistically significant difference in the ratio of center versus the periphery ratio, the total distance traveled, and the total time spent in the center of the arena between the control and knockout groups. These measures remained statistically similar between genotypes when analyzed separately by sex, as shown in Figures 8 and 9, respectively.

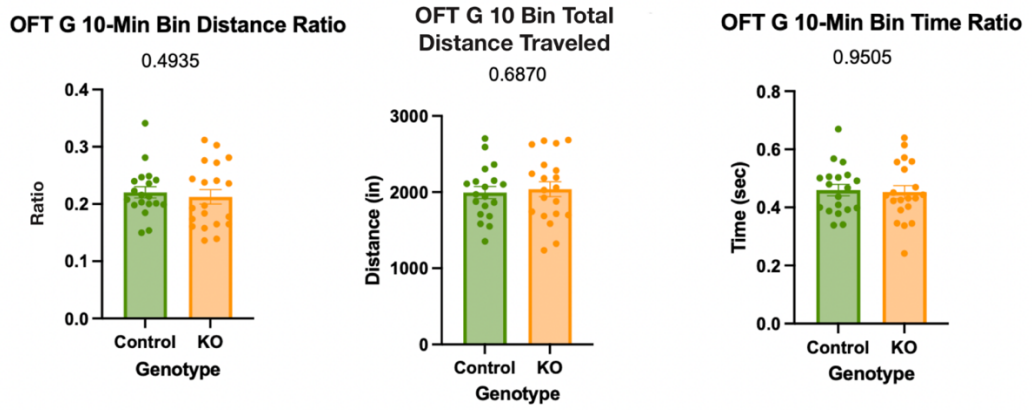

Figure 8. *Open Field test activity in control and knockout mice. Comparison of OFT activity between control and PV-Traf3 knockout mice. The graphs show the 10-minute bin distance ratio (left), total distance traveled (middle), and 10-minute bin time ratio (right). Individual points represent measurements from individual mice, while bars represent group means and error bars indicate variability. The reported p-values are shown above each graph.*

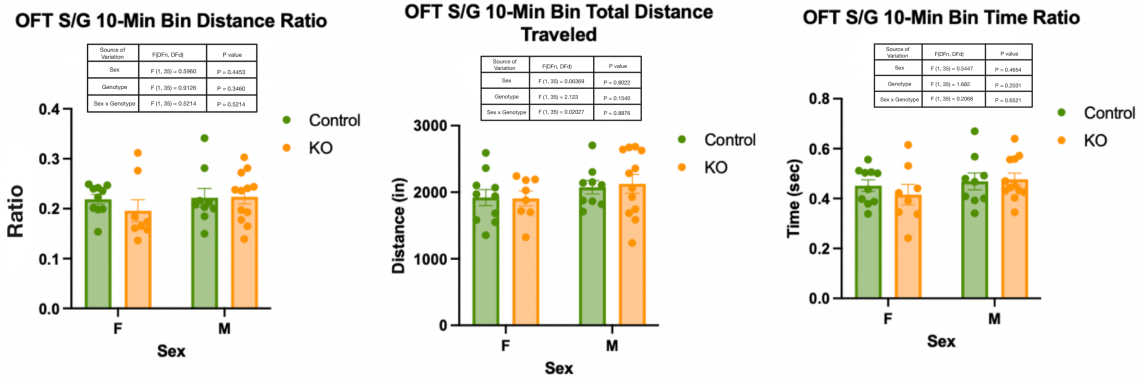

Figure 9. *Open Field test activity by sex and genotype. Comparison of OFT activity between control and PV-Traf3 knockout mice separated by sex. The graphs show the same measures as mentioned above, for female (F) and male (M) mice. Individual points represent individual mice, bars indicate group means, and error bars represent variability. The statistical analyses shown above each graph assess the effects of sex, genotype, and the sex x genotype interaction with the corresponding F- and p-values displayed.*

Elevated Plus Maze

We did not observe any statistically significant difference in the ratio of distance traveled in the open arms versus the closed arms, the total distance traveled, and the ratio of total time spent in the open arms versus the closed arms. These measures remained statistically similar between genotypes when analyzed separately by sex, as shown in Figures 10 and 11, respectively.

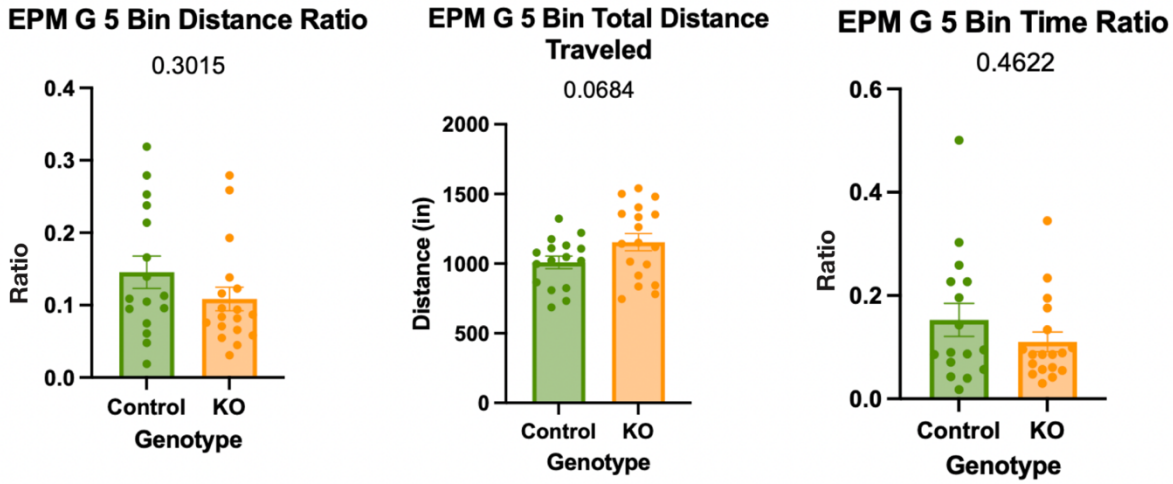

Figure 10. *Elevated Plus Maze test activity in control and knockout mice. Comparison of EPM activity between control and PV-Traf3 knockout mice. The graphs show the 5-minute bin distance ratio (left), total distance traveled (middle), and 5-minute bin time ratio (right). Individual points represent individual mice, bars indicate group means, and error bars represent variability. The p-values for the comparisons are shown above each graph.*

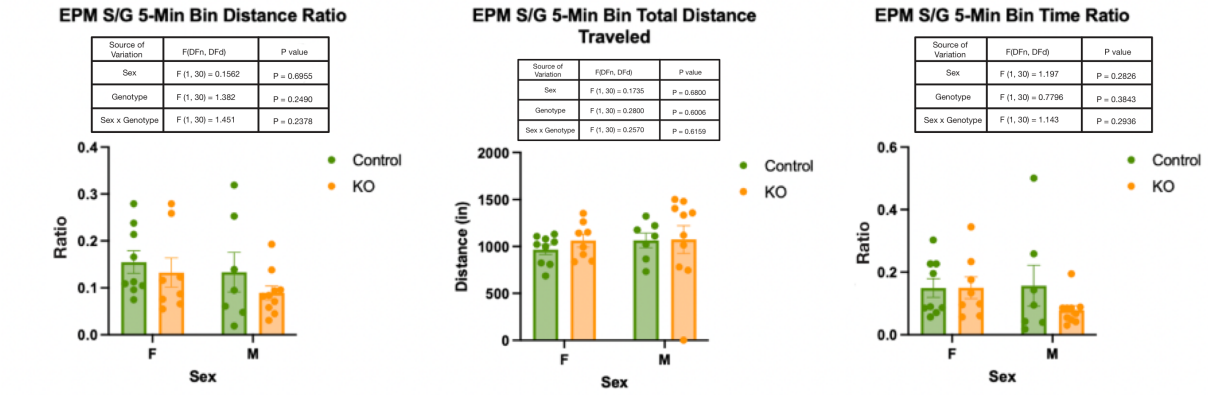

Figure 11. *Elevated Plus Maze test activity by sex and genotype. Comparison of elevated plus maze (EPM) activity between control and PV-Traf3 knockout mice, separated by sex. The graphs show the 5-minute bin distance ratio (left), total distance traveled (middle), and 5-minute bin time ratio (right) for female (F) and male (M) mice. Individual points represent individual mice, bars indicate group means, and error bars represent variability. Statistical analysis was used to assess the effects of sex, genotype, and the sex × genotype interaction, with corresponding F-values and p-values shown above each graph,*

Fear Conditioning

During fear conditioning, freezing increased across the conditioning events, which indicates the association formation between the cue (tone) and aversive stimulus (foot shock) (event effect: $p < 0.0001$). However, there was no significant effect of genotype ($p = 0.9844$) and no significant sex × genotype interaction ($p = 0.5813$), indicating that control and KO mice did not differ significantly in their acquisition of conditioned freezing. During cued fear retrieval on Day 1, freezing also differed significantly across cue presentations. There was no significant effect of genotype ($p = 0.1784$) or sex × genotype ($p = 0.9192$).

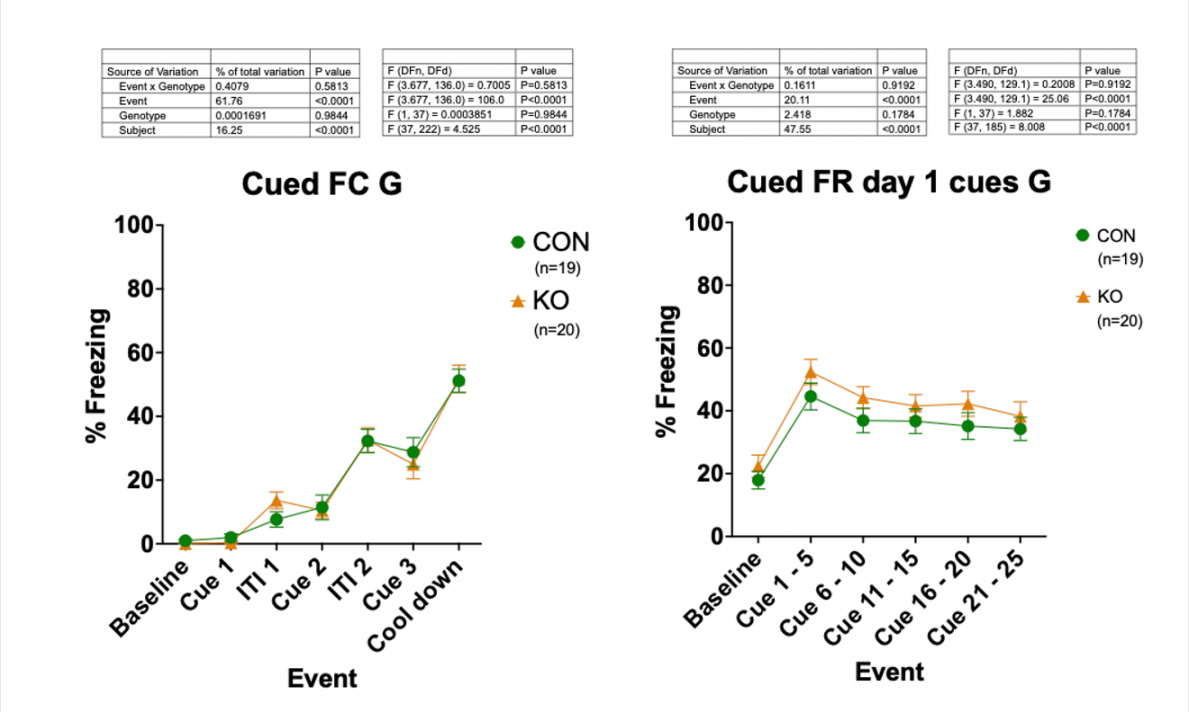

Figure 12. *Fear conditioning and retrieval in control and knockout mice. The graphs show percentage freezing in control (CON, green) and PV-Traf3 KO (KO, orange) mice during fear conditioning (Cued FC G, left) and the first day of cued fear retrieval (Cued FR day 1 cues G, right). Data are presented as mean and their error bars. Statistical analyses examined the effects of event, genotype, and event × genotype interaction, with F-values and corresponding p-values shown above each graph.*

Discussion and Future Directions

The primary objective of this study was to determine whether the anxiety- and depression-like phenotypes observed in the vGat-Traf3 KO are specifically driven by PV INs. Using the conditional PV-Traf3 KO mouse model, the baseline anxiety-like behavior and fear conditioning dynamics were evaluated.

Based on the absence of baseline behavioral phenotypes in the PV-Traf3 KO subjects observed in the OFT and EPM, it was proven that the selective deletion of Traf3 in PV

interneurons did not recapitulate the behavioral differences seen in the global vGat-Traf3 KO mice. In both the OFT and EPM, PV-Traf3 KO animals exhibited no significant differences (p-value > 0.05) compared to controls across total distance traveled, center time ratios, or open arm exploration. These findings indicate that Traf3 expression strictly within PV INs is not required for maintaining baseline anxiety levels.

Similarly, PV-Traf3 KO mice displayed intact fear acquisition and extinction recall. While vGat-Traf3 KO mice showed elevated freezing during both conditioning acquisition and initial recall, the conditional PV-Traf3 KO did not follow this. Both control and knockout cohorts demonstrated similar learning during the acquisition and extinction periods of the fear conditioning protocol. Statistical tests confirmed that there were no statistically significant genotype or genotype-by-event interaction effects on either fear acquisition or extinction. The difference in the two KO models suggests that the increased fear response observed in broad vGat-Traf3 knockouts does not depend on the absence of Traf3 from PV INs.

These results could be attributed to several reasons. The behavioral differences between the vGat-Traf3 KO and the PV-Traf3 KO mice may be driven by distinct windows of gene deletion. While vGat expression begins early during embryonic interneuron development (Saito et al. 2010), PV expression occurs later in postnatal development (P13 - P14) (Carlén et al. 2012). Thus, it is possible that Traf3 plays a fundamental role in early neurodevelopmental processes, which would occur before PV gene expression switched on. Because Traf3 expression remains intact throughout embryonic and early postnatal development in the PV-Traf3 KO mice, critical circuit maturation likely proceeds normally during this window. This preservation could explain why these mice, which were tested at 12 weeks old, don't exhibit the same anxiety and fear acquisition deficits observed in the broad vGat-Traf3 KO mice. Alternatively, the behavioral

phenotype seen in the vGat-Traf3 KO mice may be driven by a different interneuron subtype altogether. As explained previously, the vGat promoter targets all inhibitory neurons, which encompasses not only PV INs, but also SST and VIP INs. It could be that Traf3 disruption within another IN subtype drives these behavioral phenotypes, or that a concurrent disruption or loss across multiple IN populations is required to elicit phenotypes.

Overall, this project revealed that the behavioral phenotype and increased fear response observed in the vGat-Traf3 KO mice are not directly attributed to Traf3 deletion within PV INs. However, to clarify these findings, the laboratory's next step will be to validate the efficiency of Traf3 knockout specifically in PV neurons in the PV-Traf3 KO model. If validation testing reveals incomplete or unsuccessful recombination at 12 weeks, performing the behavioral battery in older mice may be suitable. If Traf3 PV-specific deletion efficiency is confirmed, future work should pivot toward isolating other distinct IN subtypes. Targeted knockouts in SST or VIP INs will be essential to determine whether another specific IN subtype drives the behavioral phenotype previously observed in the broad vGat model.

References

Bygrave, Alexei M., Ayesha Sengupta, Ella P. Jackert, Mehroz Ahmed, Beloved Adenuga, Erik Nelson, Hana L. Goldschmidt, Richard C. Johnson, Haining Zhong, Felix L. Yeh, Morgan Sheng, and Richard L. Huganir. 2023. "Btbd11 Supports Cell-Type-Specific Synaptic Function." *Cell Reports* 42(6):112591. doi:10.1016/j.celrep.2023.112591.

Carlén, M., K. Meletis, J. H. Siegle, J. A. Cardin, K. Futai, D. Vierling-Claassen, C. Rühlmann, S. R. Jones, K. Deisseroth, M. Sheng, C. I. Moore, and L. H. Tsai. 2012. "A Critical Role for NMDA Receptors in Parvalbumin Interneurons for Gamma Rhythm Induction and Behavior." *Molecular Psychiatry* 17(5):537–48. doi:10.1038/mp.2011.31.

Fishell, Gord, and Adam Kepecs. 2020. "Interneuron Types as Attractors and Controllers." *Annual Review of Neuroscience* 43:1–30. doi:10.1146/annurev-neuro-070918-050421.

Heo, Seok, Shiyu Zhang, Dong-Gi Mun, Akhilesh Pandey, Alexei M. Bygrave, and Richard L. Huganir. 2026. "Sex- and Experience-Dependent Regulation of Synaptic Protein Turnover." *Proceedings of the National Academy of Sciences* 123(28):e2602111123. doi:10.1073/pnas.2602111123.

Kimbrel, Nathan A., Melanie E. Garrett, Mariah K. Evans, Clara Mellows, Michelle F. Dennis, Lauren P. Hair, Michael A. Hauser, the VA Mid-Atlantic MIRECC Workgroup, Allison E. Ashley-Koch, Jean C. Beckham, Patrick S. Calhoun, Eric Dedert, Eric B. Elbogen, John A. Fairbank, Robin A. Hurley, Jason D. Kilts, Nathan A. Kimbrel, Angela Kirby, Sarah L. Martindale, Christine E. Marx, Scott D. McDonald, Scott D. Moore, Rajendra A. Morey, Jennifer C. Naylor, Jared Rowland, Robert D. Shura, Cindy Swinkels, Larry A. Tupler, Elizabeth E. Van Voorhees, and Ruth Yoash-Gantz. 2023. "Large Epigenome-Wide Association Study Identifies Multiple Novel Differentially Methylated CpG Sites

Associated with Suicidal Thoughts and Behaviors in Veterans." *Frontiers in Psychiatry* 14. doi:10.3389/fpsyt.2023.1145375.

Levey, Daniel F., Murray B. Stein, Frank R. Wendt, Gita A. Pathak, Hang Zhou, Mihaela Aslan, Rachel Quaden, Kelly M. Harrington, Yaira Z. Nuñez, Cassie Overstreet, Krishnan Radhakrishnan, Gerard Sanacora, Andrew M. McIntosh, Jingchunzi Shi, Suyash S. Shringarpure, John Concato, Renato Polimanti, and Joel Gelernter. 2021. "Bi-Ancestral Depression GWAS in the Million Veteran Program and Meta-Analysis in >1.2 Million Subjects Highlights New Therapeutic Directions." *Nature Neuroscience* 24(7):954–63. doi:10.1038/s41593-021-00860-2.

Luo, Xiangli, Zhan Wang, Jiancheng Xu, Zhao Gao, Zhengdong Song, and Wenji Wang. 2024. "SNHG7 Regulates Spinal Cord Injury-Induced Inflammatory Response, Oxidative Stress, and Apoptosis via the miR-199b-5p/TRAF3 Axis." *Minerva Medica* 115(3). doi:10.23736/S0026-4806.23.08689-5.

Mark &Eacute, Czeisler, M. A. Rashon I. Lane, M. D. Emiko Petrosky, PhD Joshua F. Wiley, M. P. H. Aleta Christensen, PhD Rashid Njai, PhD Matthew D. Weaver, PhD Rebecca Robbins, PhD Elise R. Facer-Childs, PhD Laura K. Barger, M. D. Charles A. Czeisler, Mbbs Mark E. Howard, and PhD Shantha M. W. Rajaratnam. 2020. "Mental Health, Substance Use, and Suicidal Ideation During the COVID-19 Pandemic — United States, June 24–30, 2020." *MMWR. Morbidity and Mortality Weekly Report* 69. doi:10.15585/mmwr.mm6932a1.

McIntyre, Roger S., Mohammad Alsuwaidan, Bernhard T. Baune, Michael Berk, Koen Demyttenaere, Joseph F. Goldberg, Philip Gorwood, Roger Ho, Siegfried Kasper, Sidney H. Kennedy, Josefina Ly-Uson, Rodrigo B. Mansur, R. Hamish McAllister-Williams,

James W. Murrough, Charles B. Nemeroff, Andrew A. Nierenberg, Joshua D. Rosenblat, Gerard Sanacora, Alan F. Schatzberg, Richard Shelton, Stephen M. Stahl, Madhukar H. Trivedi, Eduard Vieta, Maj Vinberg, Nolan Williams, Allan H. Young, and Mario Maj. 2023. "Treatment-resistant Depression: Definition, Prevalence, Detection, Management, and Investigational Interventions." *World Psychiatry* 22(3):394–412. doi:10.1002/wps.21120.

Nievergelt, Caroline M., Adam X. Maihofer, Elizabeth G. Atkinson, Chia-Yen Chen, Karmel W. Choi, Jonathan R. I. Coleman, Nikolaos P. Daskalakis, Laramie E. Duncan, Renato Polimanti, Cindy Aaronson, Ananda B. Amstadter, Soren B. Andersen, Ole A. Andreassen, Paul A. Arbisi, Allison E. Ashley-Koch, S. Bryn Austin, Esmina Avdibegoviç, Dragan Babić, Silviu-Alin Bacanu, Dewleen G. Baker, Anthony Batzler, Jean C. Beckham, Sintia Belangero, Corina Benjet, Carisa Bergner, Linda M. Bierer, Joanna M. Biernacka, Laura J. Bierut, Jonathan I. Bisson, Marco P. Boks, Elizabeth A. Bolger, Amber Brandolino, Gerome Breen, Rodrigo Affonseca Bressan, Richard A. Bryant, Angela C. Bustamante, Jonas Bybjerg-Grauholm, Marie Bækvad-Hansen, Anders D. Børglum, Sigrid Børte, Leah Cahn, Joseph R. Calabrese, Jose Miguel Caldas-de-Almeida, Chris Chatzinakos, Sheraz Cheema, Sean A. P. Clouston, Lucía Colodro-Conde, Brandon J. Coombes, Carlos S. Cruz-Fuentes, Anders M. Dale, Shareefa Dalvie, Lea K. Davis, Jürgen Deckert, Douglas L. Delahanty, Michelle F. Dennis, Frank Desarnaud, Christopher P. DiPietro, Seth G. Disner, Anna R. Docherty, Katharina Domschke, Grete Dyb, Alma Džubur Kulenović, Howard J. Edenberg, Alexandra Evans, Chiara Fabbri, Negar Fani, Lindsay A. Farrer, Adriana Feder, Norah C. Feeny, Janine D. Flory, David Forbes, Carol E. Franz, Sandro Galea, Melanie E. Garrett, Bizu Gelaye, Joel Gelernter,

Elbert Geuze, Charles F. Gillespie, Slavina B. Goleva, Scott D. Gordon, Aferdita Goçi, Lana Ruvolo Grasser, Camila Guindalini, Magali Haas, Saskia Hagenaars, Michael A. Hauser, Andrew C. Heath, Sian M. J. Hemmings, Victor Hesselbrock, Ian B. Hickie, Kelleigh Hogan, David Michael Hougaard, Hailiang Huang, Laura M. Huckins, Kristian Hveem, Miro Jakovljević, Arash Javanbakht, Gregory D. Jenkins, Jessica Johnson, Ian Jones, Tanja Jovanovic, Karen-Inge Karstoft, Milissa L. Kaufman, James L. Kennedy, Ronald C. Kessler, Alaptagin Khan, Nathan A. Kimbrel, Anthony P. King, Nastassja Koen, Roman Kotov, Henry R. Kranzler, Kristi Krebs, William S. Kremen, Pei-Fen Kuan, Bruce R. Lawford, Lauren A. M. Lebois, Kelli Lehto, Daniel F. Levey, Catrin Lewis, Israel Liberzon, Sarah D. Linnstaedt, Mark W. Logue, Adriana Lori, Yi Lu, Benjamin J. Luft, Michelle K. Lupton, Jurjen J. Luykx, Iouri Makotkine, Jessica L. Maples-Keller, Shelby Marchese, Charles Marmar, Nicholas G. Martin, Gabriela A. Martínez-Levy, Kerrie McAloney, Alexander McFarlane, Katie A. McLaughlin, Samuel A. McLean, Sarah E. Medland, Divya Mehta, Jacquelyn Meyers, Vasiliki Michopoulos, Elizabeth A. Mikita, Lili Milani, William Milberg, Mark W. Miller, Rajendra A. Morey, Charles Phillip Morris, Ole Mors, Preben Bo Mortensen, Mary S. Mufford, Elliot C. Nelson, Merete Nordentoft, Sonya B. Norman, Nicole R. Nugent, Meaghan O'Donnell, Holly K. Orcutt, Pedro M. Pan, Matthew S. Panizzon, Gita A. Pathak, Edward S. Peters, Alan L. Peterson, Matthew Peverill, Robert H. Pietrzak, Melissa A. Polusny, Bernice Porjesz, Abigail Powers, Xue-Jun Qin, Andrew Ratanatharathorn, Victoria B. Risbrough, Andrea L. Roberts, Alex O. Rothbaum, Barbara O. Rothbaum, Peter Roy-Byrne, Kenneth J. Ruggiero, Ariane Rung, Heiko Runz, Bart P. F. Rutten, Stacey Saenz de Viteri, Giovanni Abrahão Salum, Laura Sampson, Sixto E. Sanchez, Marcos Santoro, Carina

Seah, Soraya Seedat, Julia S. Seng, Andrey Shabalin, Christina M. Sheerin, Derrick Silove, Alicia K. Smith, Jordan W. Smoller, Scott R. Sponheim, Dan J. Stein, Synne Stensland, Jennifer S. Stevens, Jennifer A. Sumner, Martin H. Teicher, Wesley K. Thompson, Arun K. Tiwari, Edward Trapido, Monica Uddin, Robert J. Ursano, Unnur Valdimarsdóttir, Miranda Van Hooff, Eric Vermetten, Christiaan H. Vinkers, Joanne Voisey, Yunpeng Wang, Zhewu Wang, Monika Waszczuk, Heike Weber, Frank R. Wendt, Thomas Werge, Michelle A. Williams, Douglas E. Williamson, Bendik S. Winsvold, Sherry Winternitz, Christiane Wolf, Erika J. Wolf, Yan Xia, Ying Xiong, Rachel Yehuda, Keith A. Young, Ross McD Young, Clement C. Zai, Gwyneth C. Zai, Mark Zervas, Hongyu Zhao, Lori A. Zoellner, John-Anker Zwart, Terri deRoon-Cassini, Sanne J. H. van Rooij, Leigh L. van den Heuvel, Murray B. Stein, Kerry J. Ressler, and Karestan C. Koenen. 2024. “Genome-Wide Association Analyses Identify 95 Risk Loci and Provide Insights into the Neurobiology of Posttraumatic Stress Disorder.” *Nature Genetics* 56(5):792–808. doi:10.1038/s41588-024-01707-9.

Products - Data Briefs - Number 361 - March 2020. 2020. https://www.cdc.gov/nchs/products/databriefs/db362.htm.

Saito, Kenzi, Toshikazu Kakizaki, Ryotaro Hayashi, Hiroshi Nishimaru, Tomonori Furukawa, Yoichi Nakazato, Shigeo Takamori, Satoe Ebihara, Masakazu Uematsu, Masayoshi Mishina, Jun-ichi Miyazaki, Minesuke Yokoyama, Shiro Konishi, Koichi Inoue, Atsuo Fukuda, Manabu Fukumoto, Kenji Nakamura, Kunihiko Obata, and Yuchio Yanagawa. 2010. “The Physiological Roles of Vesicular GABA Transporter during Embryonic Development: A Study Using Knockout Mice.” *Molecular Brain* 3:40. doi:10.1186/1756-6606-3-40.

Zhou, Yan, Tao Tao, Guangjie Liu, Xuan Gao, Yongyue Gao, Zong Zhuang, Yue Lu, Han Wang, Wei Li, Lingyun Wu, Dingding Zhang, and Chunhua Hang. 2021. “TRAF3 Mediates Neuronal Apoptosis in Early Brain Injury Following Subarachnoid Hemorrhage via Targeting TAK1-Dependent MAPKs and NF-κB Pathways.” *Cell Death & Disease* 12(1):10. doi:10.1038/s41419-020-03278-z.